Academic Article

Effects of windows with heat ray retro-reflective film on outdoor thermal environment and building cooling load

Shinji Yoshida*[1] Saori Yumino *[2] Taiki Uchida *[3] Akashi Mochida*[4]

*[1]Associate Professor, Faculty of Engineering, University of Fukui
*[2] JSPS research fellow, Dept. of Architecture and Building Science, Graduate School of Engineering, Tohoku University
*[3] Graduate Student, Dept. of Architecture and Building Science, Graduate School of Engineering, Tohoku University
*[4] Professor, Dept. of Architecture and Building Science, Graduate School of Engineering, Tohoku University

Corresponding author: Shinji YOSHIDA, y-shinji@u-fukui.ac.jp

ABSTRACT

This study aimed to compare the effects of a heat ray retro-reflective film and other countermeasure techniques for windows, from the perspective of reducing the cooling load and mitigating the effects on thermal environment. In this study, we simulated the radiation field around an isolated building during the summer season using a method that considers the directional reflection. Four different windows installed on the building surface were compared: (1) single float glass with a heat ray retro-reflective film, (2) untreated single float glass, (3) single float glass with heat-shading film, and (4) low-e double glass. Through comparison, it was clarified that the adoption of the heat ray retro-reflective film on the building surface improved the radiant environment in outdoor space and reduced the cooling load during the summer season.

Key Words : Urban heat island, Retro-reflective film, Energy saving

1. Introduction

Recently, various countermeasures have been launched to combat urban warming. There are three perspectives of countermeasures of urban warming: mitigating global warming, mitigating urban heat island, and adapting to urban warming[(1)(2)]. However, their distinction remains unclear among researchers. For example, low-e double glazing and heat shading films have become popular for reducing building cooling load. Thus, adopting these countermeasures has a positive impact on mitigating global warming; however, it has a negative impact on adapting to urban warming because reflected solar radiation from a building surface worsens outdoor thermal environment (Fig.1). Hence, in this example, simultaneous evaluation of the two perspectives (mitigating global warming and adapting to urban warming) is important in selecting the proper countermeasures against urban warming.

In recent years, heat ray retro-reflective films for window application have been attracting attention. It is expected that the adoption of this film will have a positive impact through reduction in the cooling load and mitigation of the effects on thermal environment in outdoor spaces, as shown in Fig.1.

The aim of this study was to compare the effects of the heat ray retro-reflective film and other countermeasure techniques for windows on thermal environment and the cooling load simultaneously.

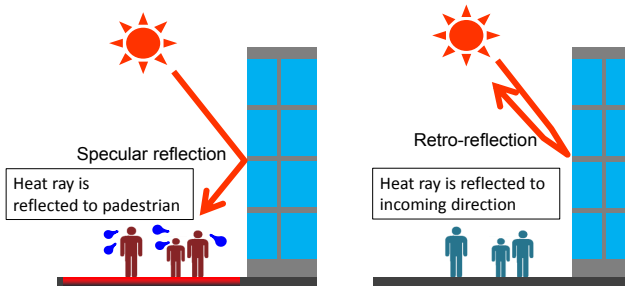

(1) previous heat shading films (2) retro-reflective film

Fig.1: Difference of a retro-reflective film and previous heat shading films

2. Outline of radiant analysis considering directional reflection

2.1 Definition of elevation and azimuth angles

Figure 2 illustrates a local coordinate system on a surface element i in order to define an elevation and an azimuth angle in this study. The elevation angle θ is defined as the angle between

the normal line to the surface element i and the incident/reflective heat ray. Hence, $\theta = 0°$ is normal to i, while $\theta = 90°$ is a tangent to i. The azimuth angle φ is defined as the angle between the X-axis in the local coordinate and the incident/reflective heat ray, with counter clockwise rotation taken to be a positive angle. In the field of building environmental engineering, the angle for which rotation is clockwise is defined as the azimuth A_z, as shown in Fig. 2. However, in mathematical coordinates, the former angle (φ) is more readily available. Hence, both definitions are used together in the present paper.

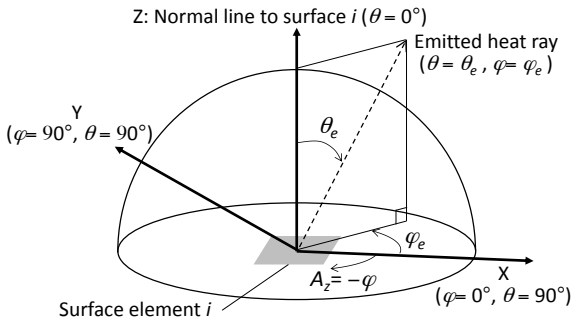

Fig.2: Definition of an elevation and an azimuth angle in a local coordinate system on a surface element i.

2.2 Existing method for radiant computation

Many researchers have developed and used radiant simulation to evaluate the effects of radiation on thermal environment in outdoor space. In most of these methods, radiosity, or the total radiation energy flux leaving a surface per unit area and unit time, is defined by Eq. (1):

$$R_i = E_i + \rho_i \sum_{j=1}^{N} F_{ji} R_j \quad (1)$$

where R_i is the radiosity [W], ρ_i is the reflectance of the surface element i, E_i is the radiation emitted at the surface element i [W], and F_{ij} is the form factor, i.e. the fraction of radiation leaving the surface element i that is intercepted by a surface element j. In this method, each surface in the computational domain is assumed to be a perfectly diffusively reflecting (or Lambertian) surface. Hence, the radiosity of surface element i intercepted by a surface element j per unit of solid angle $R_{i(j)}$ is defined by the following equation:

$$R_{i(j)} = R_i / \pi \quad (2)$$

As shown in the Eqs. (2), most of the existing methods could not evaluate the radiant field that is strongly affected by the directional reflection, such as the radiant field around a window with a heat ray retro-reflective film.

2.3 The equations of the radiant computation considering directional reflective property

In this study, to consider the directional reflection, radiant heat exchanges between urban surfaces were calculated by a method proposed by Yoshida et al.[3]. This method is revised the progressive radiosity method extended to the directional radiant computation[4] for outdoor space.

The equations of the expanded radiosity method are as follows:

$$R_{i(j)} = E_{i(j)} + \sum_{k=1}^{N} \kappa_{ki} F_{ki} \cdot \rho_{ki(j)} \cdot \pi \cdot R_{k(i)} \quad (3)$$

$$\kappa_{ki} = \rho_{hemi(k,i)} / \sum_{j=1}^{N} F_{ij} \cdot \pi \cdot \rho_{ki(j)} \quad (4)$$

where $R_{i(j)}$ is the radiosity per unit solid angle of surface element i intercepted by a surface element j [W/sr], $E_{i(j)}$ is the radiation per unit solid angle emitted from surface i to surface j [W/sr], $\rho_{ki(j)}$ is the fraction of the radiosity reaching surface j from surface k via surface i per unit solid angle [1/sr], κ_{ki} is the correction coefficient of the distribution of the reflected radiosity from surface k to surface i, and $\rho_{hemi(k,i)}$ is the reflectivity measurement value from surface k via surface i to the surroundings.

In this study, we incorporate this method into the analysis of the spatial distributions of solar radiation. In this case, $E_{i(j)}$ is the sum of the reflective components of incident, direct, and diffusive solar radiation at surface i to j:

$$E_{i(j)} = \rho_{(\theta_S, \varphi_S; i,j)} E_{Di} + \sum_{k=1}^{N_{sky}} \kappa_{ki} \rho_{ki(j)} A_i F_{ik} I_{SH} \quad (5)$$

where θ_S and φ_S are the elevation and the azimuth angle of the sun's rays to the plane, respectively, E_{Di} is the direct solar radiation gain to surface i [W], N_{sky} is the number of surface elements that comprise the sky area, A_i is the area of surface i, and I_{SH} is the incident sky solar radiation on a horizontal surface [W/m^2].

2.4 Calculation of directional reflectivity per unit solid angle

In the method described in sections 2.2 and 2.3, the distributions of directional reflectivity per unit solid angle $\rho_{i,j(k)}$ affect the calculation results considerably. Ichinose et al. (2005) set $\rho_{i,j(k)}$ using the Anisotropic body of rotation of the Normal Distribution function (AND) model that was proposed by Makino et al. (1999) [5]. In this study, we adopt the AND model for the calculation of $\rho_{i,j(k)}$ for the heat ray retro-reflective film applied to windows.

In the AND model, the total directional reflectivity per unit solid angle $\rho(\theta_i; \theta_o; \varphi_o)$ is divided into a directional and a diffusive component of reflectivity as shown in Eq. (6):

$$\rho_{(\theta_i;\theta_o;\varphi_o)} = \rho_{D_{(\theta_i)}} + \rho_{S(\theta_i;\theta_o;\varphi_o)} \quad (6)$$

where $\rho_D(\theta_i)$ is the diffusive reflectivity per unit solid angle at the incident elevation angle θ_i [1/sr]. The symbol $\rho_S(\theta_i; \theta_o; \varphi_o)$ is the directional reflectivity per unit solid angle at the incident elevation

angle θ_i, the reflect elevation angle θ_o, and the reflect azimuth angle φ_o [1/sr].

Then, $\rho_S(\theta_i;\ \theta_o;\ \varphi_o)$ is calculated using Eqs. (7), (8), (9), (10), (11), and (12):

$$\rho_{S(\theta_i;\theta_o;\varphi_o)}cos\theta_o = A \cdot exp(-f^2/2\sigma^2)\cos\{(\pi/2)(f/g)^2\} \quad (7)$$

$$f = \sqrt{(p^2+q^2)} \quad (8)$$

$$g = (kp + \sqrt{f^2 - k^2q^2})/f \quad (9)$$

$$p = \sin\theta_o \cos(\varphi_o - \varphi_{o(max)}) - k \quad (10)$$

$$q = \sin\theta_o \sin(\varphi_o - \varphi_{o(max)}) \quad (11)$$

$$k = \sin\theta_{o(\max)} \quad (12)$$

(in the case that $\theta_o = \theta_{o(\max)}$ and $\varphi_o = \varphi_{o(\max)}$, $f = 0$; g = (a real value) $\neq$ 0),

where $\theta_{o(\max)}$ and $\varphi_{o(\max)}$ are the elevation and the azimuth angle for the maximum value of $\rho_S(\theta_i;\ \theta_o;\ \varphi_o)$, respectively. The symbol σ is a representative value for the peak width of $\rho_S\cos\theta_o$. The symbols A, ρ_D, ρ_S, σ, $\theta_{o(\max)}$, and $\varphi_{o(\max)}$ are parameters that should be set according to the characteristics of the material surface.

3. Radiation analysis for an isolated building

3.1 Study area

We investigated the effects of the heat ray retro-reflective film on the radiant thermal environment around a building and the building cooling load during the summer season.

Figure 3 illustrates the computational domain in the present analysis. As a first step of the study, it was assumed that the building is located in an area without any effects of complex terrain or locations of other buildings. The window was installed only on the western surface of the building, and the window ratio was set to 80%. In this analysis, we evaluated differences in the radiant environment due to changes in the window properties on this surface.

3.2 Meteorological conditions

We investigated the thermal environment on a particularly hot summer day. The meteorological data measured at the Japan

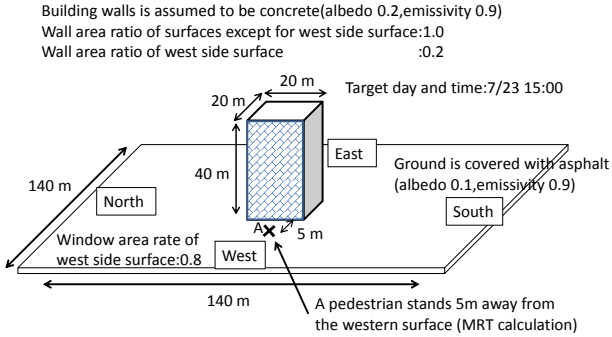

Fig.3: Computational domain in the present analysis

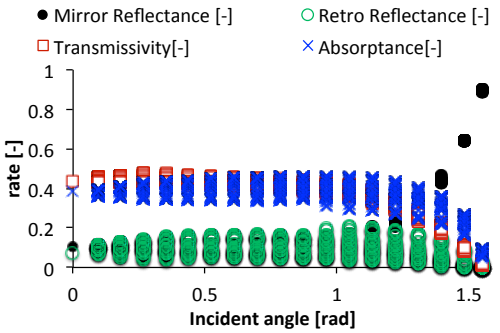

(1) Case 1

(single float glass with heat ray retro-reflective film, AND model)

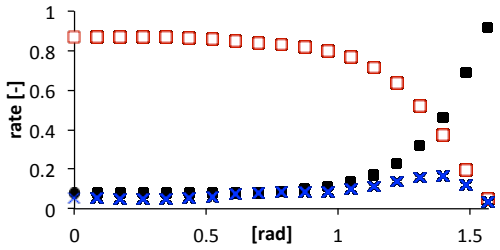

(2) Case 2 (single float glass, AND model)

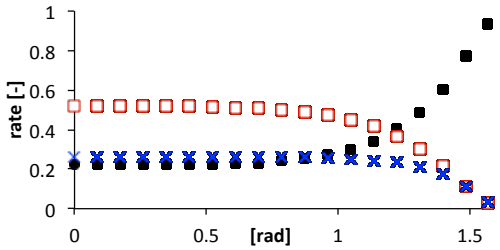

(3) Case 3

(single float glass with heat shading film, AND model)

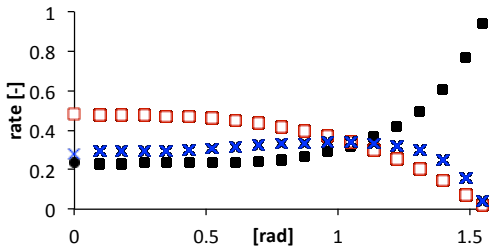

(4) Case 4 (low-e double glass, AND model)

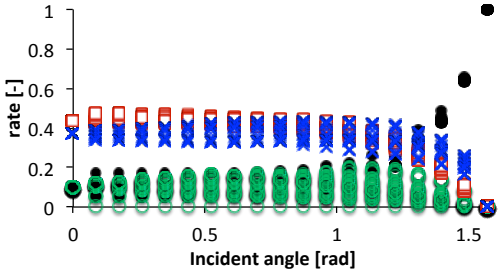

(5) Case 1

(single float glass with heat ray retro-reflective film, measurement data)

Fig.4: Distributions of absorptance, reflectance, transmissivity on each incident elevation angle to window

Meteorological Agency in Tokyo were used in this study, and the target date was set to July 23, 2010.

3.3 Computational cases

In this study, the following four computational cases were investigated. In Case 1, it was assumed that the single float glass with a heat ray retro-reflective film was used for the western window of the building, while the single float glass was used in Case 2. The single float glass with heat shading film was used in Case 3, and low-e double glass was evaluated in Case 4. In the present analysis, we model the radiant properties of these windows using the AND model according with experimental results for each window. Figure 4 illustrates distributions of absorptance, transmissivity, mirror and retro reflectance on the incident elevation angles of each case calculated by the AND model. In this figure, the experimenatl measurement data for Case 1 is also included. We can see that there is a relatively wide variation of values in Case 1. This is due to the fact that the radiant property of the heat ray retro-reflective film is affected by the incident azimuth as well as the incident elevation angle, while the other windows are only affected by the incident elevation angle.

3.4 Results

In this section, we evaluate effects of installing the window with the heat ray retro-reflective film using the results obtained at 15:00 on July 23, as a first step of this study. Solar position at this time was nearly west, and solar altitude and azimuth were approximately 46° and 83°, respectively. Under normal circumstance, the study of temporal and seasonal change is required, because the radiant property of the window depends on the incident angle of the sun ray. Hence we plan to study it in the next step of this study.

3.4.1 Radiant properties of the western surface with window

Table 1 summarizes comparisons of radiant properties between the western surfaces with windows in each case at the target time of the present analysis. The values are estimated from radiant amounts of the calculation results described in the following sections. The value of the reflectance of mirror component in Case 1 is 7.5%, while the values in Cases 2, 3, and 4 are 13.0%, 26.0%, and 26.0%, respectively. In Case 1, the value of the reflectance of retro component that is reflected to the sky is also 12.1%. Hence, we can see the window with heat ray retro-reflective film contibute to approximately 12% decrese

Table 1: Comparison of solar radiant properties between western surfaces with window in each case (weighted average of the radiant properties of window and wall at 15:00 on July 23).

	Case 1	Case 2	Case 3	Case 4
Reflectance of mirror component [%]	7.5	13.0	26.0	26.0
Reflectance of retro component [%]	12.1			
Absorptance [%]	51.3	21.8	40.8	40.8
Transmissivity [%]	32.5	66.0	34.6	34.6

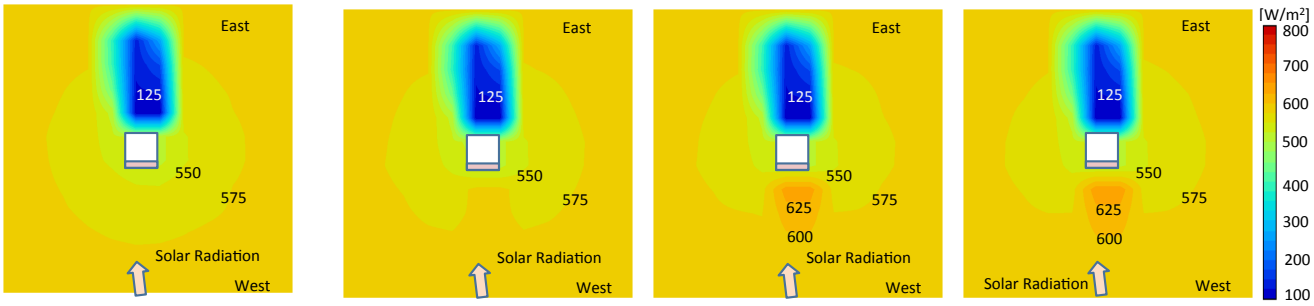

(1) Case 1 (Retro-reflective film) (2) Case 2 (The float glass) (3) Case 3 (The heat shading film) (4) Case 4 (The low-e glass)

Fig. 5: Distributions of absorbed solar radiation at 15:00 on July 23.

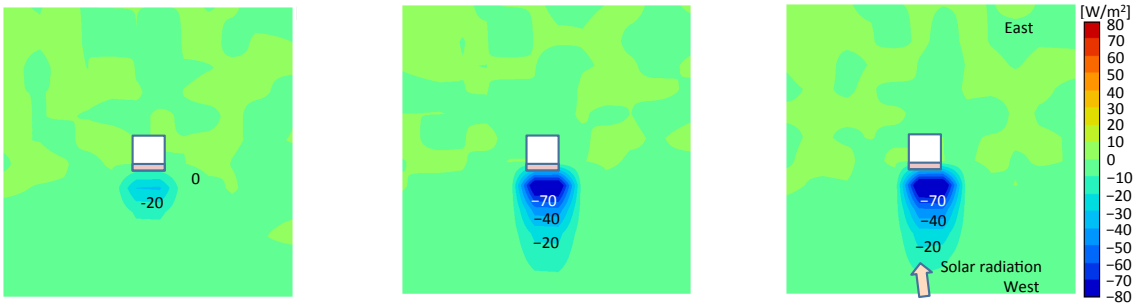

(1) Case 1 − Case 2 (Difference from the float glass) (2) Case 1 − Case 3 (Difference from the heat shading film) (3) Case 1 − Case 4 (Difference of the low-e glass)

Fig.6: Distributions of the difference between Case 1 (heat ray retro – reflective film) and other cases (at 15:00 on July 23)

in the absorbed solar radiation on the window.

3.4.2 Distributions of absorbed solar radiation

Figure 5 shows the distributions of absorbed solar radiation at the ground surface in each case. In Cases 3 and 4, the peak value of solar radiation was observed around the western surface of the building, while a peak was not observed in Case 1. For Case 1, these differences resulted from the reduction of the specular reflection component of solar radiation by adoption of the heat ray retro-reflective film.

Figure 6 shows the distributions of the difference between Case 1 and the other cases. Focusing on the difference between each case, the absorbed solar radiation around the western surface of the building in Cases 3 and 4 was larger by up to 70 W/m^2 than that for Case 1. In Case 2, the absorbed solar radiation around the western surface of the building was slightly larger than that for Case 1.

3.4.3 Evaluation of results from the perspectives of outdoor thermal environment and building cooling load

Table 2 summarizes the value of Mean Radiant Temperature (MRT) for an entire body at approximately 1 m height at point A in Fig. 3 in each case. The result of MRT was related to outdoor thermal environment for pedestrians. These values were calculated using the method for analyzing inhomogeneous radiant environments proposed by Yoshida et al. (2014) [(3)]. In this analysis, it is assumed that a pedestrian stands 5 m away from the center of the western surface of the building, as shown in Fig. 3. The pedestrian also faces to the southern direction. The height of the pedestrian is assumed to be 1.736 m. We can see the MRT in Case 1 was lower by up to 4.3°C than the MRT in Cases 3 and 4. It seems that the differences of the MRT between Case 1 and Cases 3 and 4 are not so large. It has been thought that this result has a connection with the computational domain of the present analysis. As mentioned above, in the present analysis, it is assumed that a building stands in the domain where no effects of complex terrain and other building locations are included. Hence, the results of the distributions of absorbed solar radiation and ground surface temperature are simple to understand. However, in the area where the solar radiation that is reflected from the windows is large, the amount of direct solar radiation is also large due to the simple computational domain. Hence, the influence of the direct solar radiation is dominant in most of the study area. At the next step of this study, we plan to change the study area to the building block, because the result is more complex than that of the present analysis. We expect that we can find the area where the influence of the reflected solar radiation is more dominant than that of the direct solar radiation.

Table 2 also summarises the amounts of the heat load by solar radiation transmitted into the building, and the building cooling load during the period from 15:00 to 16:00 on July 23. The amount of the transmitted solar radiation in Case 1 is approximately 520 MJ/h, while those in Cases 3 and 4 approximately 640 MJ/h and 550 MJ/h, respectively. The building cooling load in Case 1 is also approximately 1570 MJ/h, while those in Cases 3 and 4 approximately 1680 MJ/h and 1600 MJ/h, respectively. From these results, it has been found that installing the window with a heat ray retro-reflective film mitigates both the trasmitted solar radiaton and the building cooling load, compared with the window with heat shading film and the low-e double glass.

Table 2: Comparison of the MRT values and the amounts of solar radiation transmitted into the building.

	MRT at 15:00 on July 23	Heat load by solar radiation transmitted into building during the period from 15:00 to 16:00 on July 23 [MJ/h].	Building cooling load during the period from 15:00 to 16:00 on July 23 [MJ/h].
Case 1	64.4	520	1570
Case 2	64.7	1054	2059
Case 3	67.9	646	1686
Case 4	68.7	551	1602

4. Conclusions

(1) The radiant environment around a building with four different glazing types on the exterior window surface was simulated using a method that considers the directional reflection.

(2) The results indicated that the MRT around the single float glass window with the heat ray retro-reflective film was lower by up to 4.3°C than that around the low-e double glass window. The amount of solar radiation transmitted into the building with the single float glass window with the heat ray retro-reflective film was lower than that of Case 2.

(3) As a future goal of this study, the thermal environment of a real town block based on the application of the heat ray retro-reflective film will be simulated, and the effects of the film will be evaluated.

Acknowledgements

This work was supported by JSPS Grant-in-Aid for Scientific Research (B) (Grant Number 26289200) and Grant-in-Aid for JSPS Fellows.

Table of symbols

A	Maximum value of the directional reflective component	1/sr
A_i	Area of surface i	W
E_{Di}	Direct solar radiation gain to surface i	W
E_i	Radiation emitted at the surface element i	W
$E_{i(j)}$	radiation per unit solid angle emitted from surface i to surface j	W/sr
F_{ij}	Form factor for a surface element i to a surface element j	-
I_{SH}	Incident sky solar radiation on a horizontal surface	W/m^2
N_{sky}	Number of surface elements that comprise the sky area	-
R_i	Radiosity at the surface element i	W
$R_{i(j)}$	Radiosity of surface element i intercepted by a surface element j per unit of solid angle	W/sr
θ	Elevation angle	rad
θ_i	Incident elevation angle to the plane	rad
θ_o	Reflect elevation angle to the plane	rad
$\theta_{o(max)}$	Reflect elevation angle for the maximum value of $\rho_S(\theta_i; \theta_o; \varphi_o)$	rad
θ_S	elevation angle of the sun's rays to the plane	rad
κ_{ki}	Reflectance of the surface element i	-
$\rho(\theta_i; \theta_o; \varphi_o)$	Total directional reflectivity per unit solid angle at the incident elevation angle θ_i, the reflect elevation angle θ_o, and the reflect azimuth angle φ_o	1/sr
$\rho_D(\theta_i)$	Diffusive reflectivity per unit solid angle at the incident elevation angle θ_i	1/sr
$\rho_{hemi(k, i)}$	reflectivity measurement value from surface k via surface i to the surroundings	-
ρ_i	Reflectance of the surface element i	-
ρ_{kij}	fraction of the radiosity reaching surface j from surface k via surface i per unit solid angle	1/sr
$\rho_S(\theta_i; \theta_o; \varphi_o)$	directional reflectivity per unit solid angle at the incident elevation angle θ_i, the reflect elevation angle θ_o, and the reflect azimuth angle φ_o	1/sr
σ	representative value for the peak width of $\rho_S\cos\theta_o$	m
φ	Azimuth angle	rad
φ_o	Reflect azimuth angle to the plane	rad
$\varphi_{o(max)}$	Reflect azimuth angle for the maximum value of $\rho_S(\theta_i; \theta_o; \varphi_o)$	rad
φ_S	Azimuth angle of the sun's rays to the plane	rad

References

(1) Yumino, S., T. Uchida, A. Mochida, and H. Kobayashi. *Study on impacts of greening and highly reflective materials on the outdoor thermal environment and cooling loads of buildings,* The 1st International Conference on Computational Engineering and Science for Safety and Environmental Problems (2014)

(2) Sasaki, K., T. Uchida, S. Yumino, A. Mochida, and H. Kobayashi. *Comprehensive assessment on the effects of the countermeasures to mitigate global warming, mitigate UHIs, and adapt to urban warming,* The 7th Japanese-German Meetng (2014)

(3) Yoshida, S., T. Sato, and M. Oguro. *Study on evaluation of inhomogeneous outdoor thermal environment using CFD analysis method coupled with a multi-node human thermoregulation model (Part 1) Investigation of inhomogeneous radiant einvironment in outdoor space using a virtual sphere covering a human body,* Journal of Environmental Engieering, Transactions of AIJ, 705, 967-977 (2014) (in Japanese with English abstract)

(4) Ichinose, M., H. Ishino, K. Kohri, and A. Nagata. *Calculation method of radiant heat transfer with directional characteristics*, Technical papers of annual meeting of IBPSA-Japan(2005) (in Japanese with English abstract)

(5) Makino, T., A. Nakamura, and H. Wakabayashi. *Directional characteristics of radiation reflection on rough metal surfaces with description of heat transfer parameters*. The Japan society of mechanical engineering, B, **65**, 630: 324-330 (1999) (in Japanese with English abstract)

(Received Dec. 9, 2014, Accepted Dec. 27, 2014)